NASA Technical Memorandum 88341

A Verification of Unsteady Navier-Stokes Solutions Around Oscillating Airfoils

Jiro Nakamichi

September 1986

National Aeronautics and
Space Administration

NASA Technical Memorandum 88341

A Verification of Unsteady Navier-Stokes Solutions Around Oscillating Airfoils

Jiro Nakamichi, Ames Research Center, Moffett Field, California

September 1986

National Aeronautics and
Space Administration

Ames Research Center
Moffett Field, California 94035

A VERIFICATION OF UNSTEADY NAVIER-STOKES SOLUTIONS AROUND OSCILLATING AIRFOILS

Jiro Nakamichi[1]

Ames Research Center

SUMMARY

A finite-difference solution code for the two-dimensional Navier-Stokes equations has been combined with a moving-grid system. The thin layer Navier-Stokes equations with a turbulence model are solved in a time-accurate manner in order to study the unsteady aerodynamics around airfoils undergoing small amplitude pitching or heaving motions in the transonic regime. The accuracy of the solutions obtained by the use of the present moving-grid technique is investigated. The effects of the minimum grid size and the integrating time-step size on the solutions are also checked. Some of the solutions obtained by the present method are compared with experimental results.

It is demonstrated that the unsteady aerodynamics around oscillating airfoils can be predicted fairly well by the present code for cases in which the dynamic angle of attack or displacement is small.

INTRODUCTION

Several schemes for the solution of unsteady gas dynamic equations have been developed in the last decade and some of these have been used to predict the unsteady aerodynamics around oscillating airfoils.

As is well known, the unsteady flow fields can be simulated by using various levels of gas dynamic equations. At present, however, most of the numerical studies on unsteady aerodynamics are based upon the potential equation or the Euler equations, that is, inviscid flow-field models. For example, Euler solutions have been obtained by Magnus and Yoshihara (1975) and Jameson (1975). The full-potential equation has been solved and studied by Isogai (1977, 1982, 1984), and Bridgeman and Steger (1982) in 2-D and 3-D problems. The small-disturbance equation has been studied by Goorjian and Guruswamy (1984). In their studies, the predictions of the unsteady aerodynamics agree well with experiments, especially when boundary layer corrections are employed.

The inviscid unsteady transonic flow fields about oscillating airfoils can be determined at a low cost compared with obtaining the same information for viscous flow fields. So the solutions of the potential equation have already been applied

[1]Ames Associate.

to aeroelasticity problems (Isogai, 1984; Bridgeman and Steger, 1982). There are a few studies of unsteady Navier-Stokes solutions: Chyu and Davis (1984) and Chyu and Kuwahara (1982) obtained Navier-Stokes solutions around oscillating airfoils. In their studies, the shock-induced separation was numerically simulated. Considering the capability of the recent super computers, however, it is time to apply the unsteady Navier-Stokes codes to practical problems. The viscous effects on transonic airfoil response and stability are one of the major interests in aeroelasticity problems.

To describe the effects of viscosity on oscillating airfoils, the Navier-Stokes equations must be solved correctly with an appropriate moving-grid system. The purpose of this report is to show the capability of the present code (based upon ARC2D) for solving unsteady problems, especially for oscillating airfoils in the transonic regime.

In the present study, the unsteady aerodynamics around airfoils are computed by use of the thin-layer approximation. The mean angle of attack is zero and the amplitudes of the oscillations are small. In addition, the turbulence model is introduced in the computations with the assumption that the transition point is at the leading edge of the airfoil.

Some of the results obtained by the present program are compared with those obtained by experiments. Although the amplitudes of the motions are small, it has been verified that the computed results are in good agreement with experimental results. The reduced frequencies of the cases studied here are relatively low, ranging from 0.1 to 0.4, which is based upon the full chord length. The computed airfoils are NACA 0012 and NACA 64A010.

The author expresses his thanks to T. J. Barth for his offering numerical data about the hyperbolic grid around a NACA 0012 airfoil and J. Baeder for reading this manuscript.

The author also expresses his thanks to the following Ames people: Dr. J. W. McCroskey for his kind advice and helpful discussions; Dr. T. H. Pulliam for his valuable comments; and Mr. M. Inouye for his kindness during the course of this study.

THE OUTLINE OF SOLUTIONS

The Navier-Stokes equations are written in a strong conservation-law form using Cartesian coordinates. We introduce the nondimensional quantities to scale the variables ρ (density), u,v (velocities), and e (the total energy) as

$$\tilde{\rho} = \frac{\rho}{\rho_\infty}, \quad \tilde{u} = \frac{u}{a_\infty}, \quad \tilde{v} = \frac{v}{a_\infty}, \quad \tilde{e} = \frac{e}{\rho_\infty a_\infty^2} \tag{1}$$

where ∞ indicates the quantities concerning freestream. Choosing a reference length, c, which is the airfoil chord length, time t may be nondimensionalized as $\tilde{t} = ta_\infty/c$. The Reynolds number is expressed as

$$\tilde{\mu} = \frac{\mu}{\mu_\infty}, \qquad Re = \frac{\rho_\infty c a_\infty}{\mu_\infty} \tag{2}$$

Note that Re uses a_∞ and, therefore, Re based on u_∞ (the usual case for experimentally given Reynolds number) must be scaled by $M_\infty = u_\infty/a_\infty$. For the remainder of this development, the ~ will be dropped for simplicity.

Then we can write the Navier-Stokes equations in a nondimensionalized form as

$$\partial_t Q + \partial_x E + \partial_y F = Re^{-1}(\partial_x E_v + \partial_y F_v) \tag{3}$$

where

$$Q = \begin{bmatrix} \rho \\ \rho u \\ \rho v \\ e \end{bmatrix}, \qquad E = \begin{bmatrix} \rho u \\ \rho u^2 + p \\ \rho uv \\ u(e + p) \end{bmatrix}, \qquad F = \begin{bmatrix} \rho v \\ \rho uv \\ \rho v^2 + p \\ v(e + p) \end{bmatrix} \tag{4}$$

$$E_v = \begin{bmatrix} 0 \\ \tau_{xx} \\ \tau_{xy} \\ f_4 \end{bmatrix}, \qquad F_v = \begin{bmatrix} 0 \\ \tau_{xy} \\ \tau_{yy} \\ g_4 \end{bmatrix} \tag{5}$$

with

$$\begin{aligned} \tau_{xx} &= \mu(4u_x - 2v_y)/3 \\ \tau_{xy} &= \mu(u_y + v_x) \\ \tau_{yy} &= \mu(-2u_x + 4v_y)/3 \\ f_4 &= u\tau_{xx} + v\tau_{xy} + \mu Pr^{-1}(\gamma - 1)^{-1}\partial_x a^2 \\ g_4 &= u\tau_{xy} + v\tau_{yy} + \mu Pr^{-1}(\gamma - 1)^{-1}\partial_y a^2 \end{aligned} \tag{6}$$

Pressure is related to the conservative flow variables, Q, by the equation of state

$$p = (\gamma - 1)\left(e - \frac{1}{2}\rho(u^2 + v^2)\right) \tag{7}$$

where γ is the ratio of specific heats, generally set to be 1.4 for air. The speed of sound is given by $a^2 = \gamma p/\rho$ for ideal fluids. The dynamic viscosity is μ and is typically made up of a constant plus a computed turbulent eddy viscosity.

The Navier-Stokes equations (Magnus and Yoshihara, 1975) may be transformed from Cartesian coordinates to general curvilinear coordinates assuming the relations between two coordinate systems as

$$\begin{aligned} \tau &= t \\ \xi &= \xi(x,y,t) \\ \eta &= \eta(x,y,t) \end{aligned} \tag{8}$$

We can easily obtain the relation between the Cartesian derivatives and the curvilinear derivatives by use of chain rule expressions as follows:

$$\begin{bmatrix} \partial_t \\ \partial_x \\ \partial_y \end{bmatrix} = \begin{bmatrix} 1 & \xi_t & \eta_t \\ 0 & \xi_x & \eta_x \\ 0 & \xi_y & \eta_y \end{bmatrix} \begin{bmatrix} \partial_\tau \\ \partial_\xi \\ \partial_\eta \end{bmatrix} \tag{9}$$

or

$$\begin{bmatrix} \partial_\tau \\ \partial_\xi \\ \partial_\eta \end{bmatrix} = \begin{bmatrix} 1 & x_\tau & y_\tau \\ 0 & x_\xi & y_\xi \\ 0 & x_\eta & y_\eta \end{bmatrix} \begin{bmatrix} \partial_t \\ \partial_x \\ \partial_y \end{bmatrix} \tag{10}$$

where

$$\begin{aligned} \xi_x &= Jy_\eta\,, \quad & \xi_y &= -Jx_\eta\,, \quad & \xi_t &= -x_\tau\xi_x - y_\tau\xi_y \\ \eta_x &= -Jy_\xi\,, \quad & \eta_y &= Jx_\xi\,, \quad & \eta_t &= -x_\tau\eta_x - y_\tau\eta_y \end{aligned} \tag{11}$$

J is defined to be the metric Jacobian, that is, $J^{-1} = (x_\xi y_\eta - x_\eta y_\xi)$. Using the above equation and expressions, the Navier-Stokes equations are rewritten in a generalized curvilinear coordinate system

$$\partial_\tau \hat{Q} + \partial_\xi \hat{E} + \partial_\eta \hat{F} = Re^{-1}[\partial_\xi \hat{E}_v + \partial_\eta \hat{F}_v] \tag{12}$$

where

$$\hat{Q} = J^{-1}\begin{bmatrix}\rho\\ \rho u\\ \rho v\\ e\end{bmatrix}, \quad \hat{E} = J^{-1}\begin{bmatrix}\rho U\\ \rho uU + \xi_x p\\ \rho vU + \xi_y p\\ U(e + p) - \xi_t p\end{bmatrix}, \quad \hat{F} = J^{-1}\begin{bmatrix}\rho V\\ \rho uV + \eta_x p\\ \rho vV + \eta_y p\\ V(e + p) - \eta_t p\end{bmatrix} \tag{13}$$

with

$$U = \xi_t + \xi_x u + \xi_y v , \quad V = \eta_t + \eta_x u + \eta_y v \tag{14}$$

the contravariant velocities. The viscous flux terms are $\hat{E}_v = J^{-1}(\xi_x E_v + \xi_y F_v)$ and $\hat{F}_v = J^{-1}(\eta_x E_v + \eta_y F_v)$.

The stress terms, such as τ_{xx} are also transformed in terms of the ξ and η derivatives where

$$\begin{aligned}
\tau_{xx} &= \mu[4(\xi_x u_\xi + \eta_x u_\eta) - 2(\xi_y v_\xi + \eta_y v_\eta)]/3\\
\tau_{xy} &= \mu(\xi_y u_\xi + \eta_y u_\eta + \xi_x v_\xi + \eta_x v_\eta)\\
\tau_{yy} &= \mu[-2(\xi_x u_\xi + \eta_x u_\eta) + 4(\xi_y v_\xi + \eta_y v_\eta)]/3\\
f_4 &= u\tau_{xx} + v\tau_{xy} + \mu Pr^{-1}(\gamma - 1)^{-1}(\xi_x \partial_\xi a^2 + \eta_x \partial_\eta a^2)\\
g_4 &= u\tau_{xy} + v\tau_{yy} + \mu Pr^{-1}(\gamma - 1)^{-1}(\xi_y \partial_\xi a^2 + \eta_y \partial_\eta a^2)
\end{aligned} \tag{15}$$

with terms such as u_x expanded by chain rule.

In high Reynolds number flows the effects of viscosity are concentrated near rigid boundaries and in wake regions. Most of the computing efforts should be concentrated on the resolution of the boundary layer. A grid is generated which is very fine in the normal direction to the body, and is coarse in the tangential one. Even if the full Navier-Stokes equations are solved on that kind of grid, the viscous terms associated with derivatives along the body will not be resolved.

The thin-layer approximation requires that:

1. All body surfaces be mapped onto coordinate surfaces. Specifically, η = constant coordinate surfaces.

2. Grid spacing is clustered to the body surfaces such that sufficient resolution for a particular Reynolds number is obtained.

3. All the viscous derivatives in the ξ direction are neglected, while the terms in the η direction are retained. All of the inviscid terms are used.

Applying the thin-layer approximation to equations (12) and (15), the thin-layer Navier-Stokes equations are written

$$\partial_\tau \hat{Q} + \partial_\xi \hat{E} + \partial_\eta \hat{F} = Re^{-1} \partial_\eta \hat{S} \tag{16}$$

where

$$\hat{S} = J^{-1} \begin{bmatrix} 0 \\ \eta_x m_1 + \eta_y m_2 \\ \eta_x m_2 + \eta_y m_3 \\ \eta_x (u m_1 + v m_2 + m_4) + \eta_y (u m_2 + v m_3 + m_5) \end{bmatrix} \tag{17}$$

with

$$\begin{aligned} m_1 &= \mu(4\eta_x u_\eta - 2\eta_y v_\eta)/3 \\ m_2 &= \mu(\eta_y u_\eta + \eta_x v_\eta) \\ m_3 &= \mu(-2\eta_x u_\eta + 4\eta_y v_\eta)/3 \\ m_4 &= \mu Pr^{-1}(\gamma - 1)^{-1} \eta_x \partial_\eta (a^2) \\ m_5 &= \mu Pr^{-1}(\gamma - 1)^{-1} \eta_y \partial_\eta (a^2) \end{aligned} \tag{18}$$

Applying an implicit three point time differencing scheme of the form,

$$\Delta\hat{Q}^n = \frac{\theta\Delta t}{1+\phi} \frac{\partial}{\partial t} (\Delta\hat{Q}^n) + \frac{\Delta t}{1+\phi} \frac{\partial}{\partial t} \hat{Q}^n + \frac{\phi}{1+\phi} \Delta\hat{Q}^{n-1} + O\left[\left(\theta - \frac{1}{2} - \phi\right)\Delta t^2 + \Delta t^3\right] \tag{19}$$

where $\Delta\hat{Q}^n = \hat{Q}^{n+1} - \hat{Q}^n$ and $\hat{Q}^n = \hat{Q}(n\Delta t)$. The parameters θ and ϕ can be chosen to produce different schemes of either first- or second-order accuracy in time.

For $\theta = 1$ and $\phi = 0$, we have the first-order Euler implicit scheme, and for $\theta = 1$ and $\phi = 1/2$, the three point implicit scheme, respectively. By solving equation (19) using the ADI (Beam-Warming) scheme, we can get the solution in a time-accurate manner. For more detail, readers are referred to Pulliam (1984).

BOUNDARY CONDITIONS FOR UNSTEADY PROBLEMS

We need boundary conditions for each conservation-law equation. At the solid surface, the density is extrapolated from the interior boundary to the flow field. For the momentum equations, the contravariant velocity U and V are set to be zero at the body surface. At the trailing edge, the Kutta condition is applied for the

airfoil. The pressure is obtained by the normal momentum equation and the acceleration of the solid surface is taken into account as follows:

$$\rho[-x_{tt}\eta_x - y_{tt}\eta_y] - \rho U(\eta_x u_\xi + \eta_y v_\xi) = (\eta_x\xi_x + \xi_y\eta_y)p_\xi + (\eta_\xi^2 + \eta_y^2)p_\eta \qquad (20)$$

When a C-type grid is used, a part of the boundary is split. All of the quantities on the cut line which are necessary for the next time step are evaluated by averaging the quantities just above and below the cut line.

In the present study, the grid is changing during the unsteady computations: the inner boundary is moving as prescribed by a function of time although the shape of the airfoil is not changing (rigid-body motion). The far-field boundary is fixed with respect to the inertial coordinate system. The grid distribution between the inner boundary and the far-field boundary is changing.

In the present technique, the orthogonality of the grid is not maintained even though the initial grid system is orthogonal. The orthogonality condition between ξ = constant lines and the airfoil surface is important for the boundary conditions to be satisfied exactly. In our numerical experiments, however, in both cases of pitching motion and heaving motion, the violation of the grid orthogonality will not cause large errors or instability during the unsteady computations as long as the amplitude is small.

At every time step, the velocity of each grid point is computed numerically using the coordinates at the previous time step and those of the updated grid. The accelerations of the grid points on the airfoil surface are also numerically calculated in a similar manner. In the case of forced oscillations, the motion of the airfoil is prescribed as a function of time, so the velocities and accelerations can be computed analytically. However, in the present study, these quantities have been computed numerically for the purpose of checking the applicability of the program for the case of the numerical simulation of the aeroelasticity problems. In that case, the airfoil motions will not be prescribed in advance. As for the far-field boundary, uniform flow conditions are applied during the unsteady computations.

MOVING-GRID SYSTEM

For the solution of the unsteady Navier-Stokes equations, the grid should be changing with the airfoil motions. The boundary conditions must be satisfied on the moving surface at each time step. In the present study, a technique is introduced to update the grid system around an airfoil which is changing in location and attitude with respect to time.

There are two techniques for a time varying-grid system: one is based upon the rigid motion of the grid system in the inertial coordinate system, and the other is based upon the deformation of the grid between the inner boundary and the outer boundary.

In the former technique, it is not necessary to update the instantaneous grid coordinates, and we need just metrics and their derivatives concerning space and time at each time step as long as we treat rigid airfoil sections. As to the computing time and storage, there are some advantages in this rigid motion of a grid system. Steger (1978), and more recently, Jesperson (1985), for example, solved Euler equations around a heaving airfoil in a time-accurate manner using this kind of grid. This technique, however, cannot be applied to problems in which the elastic deflections of airfoils should be taken into account. In 2-D problems, rigid-motion grid seems to be enough because the airfoil sections are considered to be rigid in most cases.

On the other hand, in the latter technique, the inner boundary is changing with the motion of the airfoil while the outer boundary is at rest with respect to the inertial coordinate system. It will be applicable for aeroelasticity problems as well, although both the grid coordinates and the corresponding metrics must be updated at each time step.

An implementation of the latter technique was presented by Chyu and Kuwahara (1982) and Chyu and Davis (1984). They successfully obtained the moving grid for the computations of pitching airfoils. First, they generated the static grids for the airfoil at the extreme angle of attack positions. The grid at each time step was obtained from those at the extreme positions by spatial interpolations. The inner boundary is changing with the motion of the airfoil and the far-field boundary is fixed in the inertial coordinate system. In their technique, at least two grid systems must be stored, even in the simple case of a pitching airfoil.

In the present study, a method is proposed to generate a time-varying grid system. In this method, the grid points near the inner boundary are moving completely with the motion of the airfoil while the far-field boundary is at rest during the unsteady computations. The grid distribution between the airfoil surface and the far-field boundary is determined by an analytical function along the ξ = constant lines. From the viewpoint of the accuracy of the computations, the deformations of the grid should be minimum in the flow field. The analytical function is determined so that the deformations of the grid in the vicinity of the airfoil are small, but those in the neighborhood of far-field boundary are relatively large. In problems with elastic deflections, some special technique must be employed to specify the grid points on the airfoil surface. Once the grid distributions on the rigid or elastic airfoil are specified, the grid distributions in the field will be determined by use of an algebraic function as

$$\Delta x_{i,j} = \Delta x_i \cdot \sqrt{1 - (\eta^*)^2} \tag{21}$$

$$\Delta y_{i,j} = \Delta y_i \cdot \sqrt{1 - (\eta^*)^2} \tag{22}$$

where

$$\eta^* = 0 \; ; \qquad \eta \leq \eta_o$$

$$\eta^* = (\eta - \eta_o)/(\eta_{max} - \eta_o) \; ; \qquad \eta \geq \eta_o$$

The increments of the grid coordinates are denoted by $\Delta x_{i,j}$ and $\Delta y_{i,j}$, and Δx_i and Δy_i are the displacements of the grid points on the airfoil (and the cut line when a C-type of grid is used) in the x and y directions, respectively. A parameter η_o takes a value between 0 and η_{max} depending upon the airfoil motion of interest. Usually, a value between 0.6 and 0.7 is suitable for η_o. The vector $(\Delta x_i, \Delta y_i)$ is computed from the analytical function of t in cases of forced oscillations or obtained by use of the equations of motion of the airfoil in cases of aeroelasticity problems. The updated grid will be

$$x^n_{i,j} = x^{n-1}_{i,j} + \Delta x_{i,j} \tag{23}$$

$$y^n_{i,j} = y^{n-1}_{i,j} + \Delta y_{i,j} \tag{24}$$

The grid velocities and accelerations are computed by use of $\Delta x_{i,j}$ and $\Delta y_{i,j}$ and the new coordinates can overwrite old ones.

Other choices for updating the grid system are possible. The grid has to be changed at each time step. The computing time to update the grid system should be small, and it is desirable that the scheme of changing the grid be simple and reliable for any kind of airfoil motions.

To demonstrate the present technique, a moving grid-system is shown. The airfoil is rigid and its motion around the quarter-chord is described as

$$h = 0.0 + 0.1 \cdot \sin(\omega t + 30^0) \tag{25}$$

$$\alpha = 0.0 + 10^0 \cdot \sin(\omega t) \tag{26}$$

that is, a heaving and pitching coupled motion with amplitudes, 0.1 and 10.0 deg, respectively. Both of the amplitudes are large in order to illustrate the usefulness of the present method. The phase difference between heaving and pitching motions is 30.0 deg. The initial grid is a hyperbolic-C-type generated by use of the method of Kinsey (1984).

Unfortunately, the orthogonality condition between the body surface and the ξ-constant lines is violated in spite of the fact that the initial grid is generated so as to satisfy orthogonality. However, the grid at each time step looks very reasonable. At every $\omega t = 30°$, the grid is shown in figure 1. The grid motion is

very smooth even though both of the amplitudes of the heaving and pitching motions are relatively large.

The C-type of grid has a cut line extending from the trailing edge to the downstream boundary. At each time step, the cut line is reset smoothly so as to approximate a streamline. After setting the new cut line, the grid distribution in the region behind the trailing edge of the airfoil is specified in the same manner as prescribed above.

The computing time to update the grid at each time step is less than 7% of that for solving the flow field, including the recalculation of grid coordinates, grid velocities, grid accelerations, and other quantities necessary to compute the flow field. In the present technique, the grid pattern is deforming with the flow field. Thus, the Jacobians and the metrics at the grid points are also changing with respect to time. The changing Jacobians might have some effect on the flow computations since the present code does not take them into account. We, therefore, have to check the effect by comparing two solutions: one obtained by using a deformed moving grid, the other by using a rigid body motion grid. The results of our comparison will be shown below.

RESULTS

Some verifications of the computed results are presented. Throughout the present study, the computations are performed under the flow condition $Re = 12 \times 10^6$. The thin-layer approximation and the Baldwin-Lomax turbulence model are used assuming the transition point is at the leading edge of the airfoil. Uniform flow conditions are applied at the far field boundaries which are located ten chord lengths from the airfoil. The grid size is 159 × 51. The grids used in these studies are elliptic-C-type, except for those used to demonstrate the moving grid technique. Thus, the grid for the steady state (that is, the initial grid for unsteady computations) is generated by solving a set of nonlinear Poisson's equations. The minimum size of grid and the way of stretching the grid from inner boundary to outer boundary is chosen by specifying parameters in the equations of Sorensen (1980). It satisfies the orthogonality condition between the airfoil surface and the ξ-constant lines, though some skewness is observed, especially along the cut line after the trailing edge.

The steady state is first computed. After the steady solution is sufficiently converged, the airfoil is forced to oscillate periodically. For the steady solutions, the Euler-Implicit scheme is employed; while for unsteady solutions, the Three-Point-Implicit scheme is used. The airfoil motion and the flow field around it are simulated for three cycles. In the third cycle, the data of interest are stored. The quantities obtained in a time history are analyzed by Fourier analysis. The definitions of the steady state, in-phase component, and out-of-phase component are

$$C_p = \frac{2k}{\delta\pi} \int_{cycle} F(t)dt \tag{27}$$

$$Re[\Delta C_p] = -\frac{k}{\delta\pi} \int_{cycle} F(t)\sin(kt)dt \tag{28}$$

and

$$Im[\Delta C_p] = \frac{k}{\delta\pi} \int_{cycle} F(t)\cos(kt)dt \tag{29}$$

respectively. In the above expressions, $F(t)$, is an arbitrary function of time and δ is the amplitude of the airfoil oscillation, and k is the reduced frequency defined by

$$k = \frac{c\omega}{u_\infty} \tag{30}$$

The major capabilities of the present program to be investigated are:

1. The accuracy of the computations using the moving grid system.
2. The effects of the minimum grid size used for the unsteady computations.
3. The effect of the time integration step size.
4. Comparisons between the computational results and experimental data.

It is actually difficult to watch the pure effects of each of the above items. For example, the magnitude of the smoothing parameters which is necessary to maintain the stability of the calculations will depend on the time integration step size and the minimum grid size. However, it is useful to check the above items for the numerical studies on the unsteady viscous aerodynamics.

Fortunately, for the case of an airfoil oscillating in a rigid motion, we can alternatively use the rigid motion grid method. The Jacobian at each grid point is changing with respect to time when the present moving-grid technique is employed. However, in the case of the rigid motion grid method, it is constant. The accuracy of the solutions obtained using the present technique can be checked by comparing the two results. Two computed results are compared to check the effects of deformation of the grid using a NACA 0012 airfoil in a pitching motion around the midchord axis. The amplitude of the motion is 1.0° and the reduced frequency is 0.2 with a freestream Mach number of 0.8.

As the C_p time histories of both cases are compared, no differences can be recognized. The in-phase and the out-of-phase components for both cases are compared in figure 2(a),(b). In this figure, the results from the present method are illustrated by solid lines and those from the rigid motion grid are illustrated by dotted lines. There are no significant differences between both results in the calculations of in-phase and out-of-phase components in front of the shock wave; but, at the peak of the shock wave and behind the shock wave, there are slight discrepancies between the two results.

In the computation using the rigid motion grid, some special care was taken into account concerning the evaluation of the grid velocities. Fortunately, in the case of pitching motion, the grid velocity is computed as accurately as possible using analytical relations between the inertial coordinate system (x,y) and the coordinate system fixed on the airfoil (x*,y*). We can easily obtain the following relations when the pitching axis is chosen as the origins of both systems.

$$\frac{d\xi}{dt} = \frac{1}{2}(\dot{\theta})^2 \cdot (r^2)_\eta \tag{31}$$

$$\frac{d\eta}{dt} = -\frac{1}{2}(\dot{\theta})^2 \cdot (r^2)_\xi \tag{32}$$

where $r^2 = x^2 + y^2 = (x^*)^2 + (y^*)^2$ and θ is the instantaneous angle of attack of the airfoil given by $\theta(t) = \delta \sin t(\omega \cdot t)$

$$\begin{bmatrix} x_\xi \\ y_\xi \end{bmatrix} = \begin{bmatrix} \cos\theta(t) & -\sin\theta(t) \\ \sin\theta(t) & \cos\theta(t) \end{bmatrix} \begin{bmatrix} x^*_\xi \\ y^*_\xi \end{bmatrix} \tag{33}$$

$$\begin{bmatrix} x_\eta \\ y_\eta \end{bmatrix} = \begin{bmatrix} \cos\theta(t) & -\sin\theta(t) \\ \sin\theta(t) & \cos\theta(t) \end{bmatrix} \begin{bmatrix} x^*_\eta \\ y^*_\eta \end{bmatrix} \tag{34}$$

By use of the above relations, the calculation can be continued during the pitching motion without recalculating the grid coordinates.

In figure 3(a),(b), the change in the solutions caused by the minimum grid sizes are illustrated; one is by use of minimum grid size, 2.0×10^{-6} and the other is by 2.0×10^{-4}. The former is shown by solid lines and the latter shown by dotted lines. The experimental results are also plotted in the figures by triangles. The airfoil computed here is NACA 64A010 in a pitching motion around a quarter-chord axis with reduced frequency of 0.4 and amplitude of 1.0°. The freestream Mach

number is 0.8. The results are similar with slight differences observed ahead of the shock wave.

According to our experiences, it is sometimes difficult to get the steady-state solutions sufficiently converged when a fine grid is used. It is especially true with the computations of the NACA 64A010 airfoil using an elliptic-C-type grid. The unsteady aerodynamics will depend upon the convergence status of the steady-state solution which becomes the initial condition for the unsteady problem. Thus, the steady-state solution must be examined before starting unsteady computations.

The minimum grid size has a close correlation with the number of grid points in the boundary layer. The differences between the two solutions are due to the resolution of the boundary layer. It is clear from the present results that the finer the grid used, the better is the agreement of computational solutions with experimental data. But, it should be noted that the accuracy of the solutions will depend, not only upon the minimum grid size, but also upon the manner of stretching the grid, especially in unsteady problems. The minimum grid size of 2.0×10^{-6} is sufficient to obtain good agreement with experiments. In all of the remaining results, the minimum grid size of 2.0×10^{-6} is used.

The effect of the integrating time step size is also investigated. The two results are shown in figure 4(a),(b). The airfoil is a NACA 0012 which is in a pitching motion with reduced frequency, 0.1628. The mean angle of attack is 0° and the amplitude of the pitching motion is 2.51°. The Mach number is 0.755. One is the result obtained by use of the time integrating step size, 0.01692; the other is by use of a time integrating step size of half that size, that is, 0.00846. They are based upon the nondimensionalization of $\tilde{t} = ta_\infty/c$ and each time step size results in 3020 and 6040 iterations per cycle, respectively. The former is shown by the solid line and the latter is shown by the circles. The solutions are almost identical. For the unsteady problems, it is inevitable to adjust the smoothing parameters in the calculations because of stability reasons. In the present study, we used the minimum value of the smoothing parameters to maintain stability of the unsteady computations. The values of the smoothing parameters should be as small as possible. However, for practical computations, there will be a trade-off between the accuracy and the stability.

Figure 5 demonstrates the unsteady aerodynamics of a NACA 64A010 airfoil in a heaving motion. The reduced frequency is 0.4 and freestream Mach number is 0.8. The amplitude of the heaving motion is 0.0436 based upon the full chord length. The same problem was computed by Steger (1978) and by Jesperson (1985) using an Euler code.

In figure 6(a),(b), unsteady aerodynamic components are compared with experimental results. The case is a NACA 64A010 airfoil in a pitching motion. The reduced frequency is 0.1 and the pitching axis is a quarter chord point. The amplitude of the motion is 1.0° with a freestream Mach number, 0.8. In the figures, the experimental results are shown by circles and the computed results by solid lines. In figure 3, the solutions for the case of reduced frequency, 0.4, were already compared. In most of the experimental studies, the number of pressure orifices is

insufficient and the peak of the unsteady pressure at the shock wave cannot be captured precisely. Thus, it is somewhat difficult to compare the unsteady components of the pressure near the shock wave. As long as this fact is taken into account, both components agree fairly well with the experimental data, except for the out-of-phase component in the shock wave region. The computed results show a peak at the shock wave in the out-of-phase component while the experiment data show just a step change there. In figure 3, the same trend is observed. That is the major difference between the computed results and experiment.

Finally, a NACA 0012 airfoil is studied. The case is a NACA 0012 airfoil in a pitching motion around a quarter-chord axis. The freestream Mach number is 0.755 and the reduced frequency is 0.1628. The amplitude of the pitching motion is 2.51°, which is relatively large. In figure 7, the steady state solution is shown. The shock wave is very weak and smeared. This result compares well with the results presented in Goorjian and Guruswamy (1984). Starting with this steady-state solution, three cycles are simulated as was done in the other problems. Figure 8 shows a comparison at every 45° during the third cycle of the pitching motion. The computed results are shown by solid lines and the experimental data are plotted by daggers (†). The mean angle of attack and the Reynolds number are 0.0 and 12×10^6 in the computation; they are 0.016 and 5.5×10^6 in the experimental data (Lambourne, 1985). For this large amplitude of the pitching motion, the shock wave is relatively strong in some range of phase angle, and the unsteady component before the shock wave is very large. Thus, both components of the unsteady C_p distribution indicate no peaks at the shock wave, but present just step change at the shock location. In figure 8, most of the computed results are in excellent agreement with the experimental results, except for the part just after the shock wave. This is due to the lack of the capability of resolving the shock and boundary layer interactions.

The time history of the Mach number contours around the airfoil is illustrated in figure 9. The number of grid points is insufficient, especially around the shock wave. The interaction between the shock wave and the boundary layer cannot be observed precisely. Qualitatively, however, we can see the change of the flow field around airfoil in a cycle of motion. In figure 10, the unsteady part of the aerodynamics was obtained by Fourier analysis. However, the number of experimental data points is too small for Fourier analysis. Thus, the experimental results are not presented in the figure.

As for the sensitivity of solutions to grids, it is difficult to reach a conclusion because no single parameter can be isolated. If the grid is changed, there might be some effects even on the steady solutions. In the present study, just some of the tendencies of the solutions are shown concerning the minimum grid size as a result of number of numerical studies on unsteady Navier-Stokes solutions.

CONCLUSIONS AND DISCUSSIONS

A moving-grid technique has been demonstrated. Some of the obtained solutions have been compared with experimental results.

The present moving-grid technique is very powerful in the case of small amplitudes, and it does not increase the total computing time significantly. In the present study, both hyperbolic-C-type and elliptic-C-type grids were used. However, this moving-grid technique is applicable to other kind of grids. It has been shown that the effect of the deformations of the grid is very small and the accuracy of the solution can be retained during the unsteady computations.

The effect of minimum grid size has also been investigated. The best results were obtained when the minimum grid size of 2×10^{-6} was used. Cases may differ, but generally speaking, the finer the grid used, the better the results that are obtained. This is because the boundary layer should be resolved as accurately as possible, especially in the unsteady problems. It cannot be emphasized too strongly that most of the computing efforts should be concentrated on the resolution of the boundary layer. Some of the solutions have been shown in this report. However, it must be stressed that even the solutions which look reasonable and compare well with experimental results need more investigation concerning the boundary-layer behavior, especially for problems with shock waves.

The effect of time-integration step size has also been investigated. To obtain unsteady solutions of the Navier-Stokes equations in a finite and realistic computing time, some smoothing terms are inevitable for stability reasons. It is definitely better to use as small smoothing parameters as possible, even though a very small time step must be used for time integrations. As mentioned previously, it is a trade-off between accuracy and computing time. Fortunately, according to the present study, the solutions are independent of the time-integration step size as long as they are small enough. But, it is noted that when the time-integration step size is changed, the smoothing parameter is also adjusted to maiantain stability or accuracy.

In the Navier-Stokes computations, there are many parameters to be determined before computations. The mathematical model for the computations is determined when all of the parameters are fixed, including the grid system. The manner of stretching the grid has some effects on the unsteady solutions. In the viscous flow field, there are large dissipations. However, even an inner grid line can be a boundary for some disturbances. If the stretching is poorly done, certain waves cannot propagate through the inner grid lines and might be reflected as if from a rigid boundary. In that case, the solution will never become periodical, even if the motion of the airfoil is periodic.

The computed results were compared with experimental ones in some cases. The obtained results are more than satisfactory, but there are some disagreements about the shock wave motions. It is due to the lack of grid points around the shock wave,

and the fact that the shock wave-boundary layer interactions are not resolved adequately. Moving adaptive grid should be introduced for further investigations.

The conclusions of the present study are:

1. The accuracy of the computations can be maintained during unsteady computations using the present moving-grid technique.

2. Although it depends on requirements of accuracy, the minimum-grid size should be of the order of 10^{-6}. (Of course, it will depend on the Reynolds number.)

3. The unsteady solutions are independent of the time-integration step size as long as it is small enough.

4. The computed results are reasonable and compare well with experimental data in cases of small amplitude.

For further investigations, the following items should be addressed:

1. The sensitivity of the unsteady solutions to grids; the effects of distance to the far-field boundary and the grid stretching pattern.

2. The frequency response of the aerodynamics produced by the present program (especially in the case of small amplitude).

3. The prediction capability of shock and boundary layer interactions.

4. Computations of cases of large amplitudes.

Item 2 directly above is closely related to item 1. For practical applications, we need to develop a code which includes a systematic grid generator. Either of items 3 or 4 may be another major problem beyond the present study.

REFERENCES

Bridgeman, J. O.; and Steager, J. L.: A Conservative Finite Difference Algorithm for the Unsteady Transonic Potential Equation in Generalized Coordinates. AIAA Paper 82-1388, Aug. 1982.

Chyu, W. J.; and Davis, S. S.: Numerical Studies of Unsteady Transonic Flow Over an Oscillating Airfoil. AGARD-CP-374, Toulouse, France, Sept. 1984.

Chyu, W. J.; and Kuwahara, K.: Computations of Transonic Flow Over an Oscillating Airfoil with Shock-Induced Separation. AIAA Paper 82-0350, Jan. 1982.

Goorjian, P. M.; and Guruswamy, G. P.: Unsteady Transonic Aerodynamics and Aeroelastic Calculations About Airfoils and Wings. NASA TM-85986, Aug. 1984.

Isogai, K.: Calculation of Unsteady Transonic Flow Over Oscillating Airfoils Using the Full Potential Equation. AIAA Paper 77-448, March 1977.

Isogai, K.: Calculation of Unsteady Transonic Flow Over Oscillating Three-Dimensional Wings. TR-706T, National Aerospace Laboratory, Japan, Aug. 1982.

Isogai, K.: The Development of Unsteady Transonic 3-D Full Potential Code and Its Aeroelastic Applications. AGARD-CP-374, Toulouse, France, Sept. 1984.

Jameson, A.: Transonic Potential Flow Calculations Using Conservation Forms. 2nd AIAA Conference on Computational Fluid Dynamics, Hartford, CT, June 1975.

Jesperson, D. C.: A Time-Accurate Multiple-Grid Algorithm. AIAA Paper 85-1493-CP, July 1985.

Kinsey, W. D.: Description of a Hyperbolic Grid Generating Procedure for Arbitrary Two-Dimensional Bodies. AFWAL-TM-84-191-FIMM, July 1984.

Lambourne, N.: Compendium of Unsteady Aerodynamic Measurements. AGARD Report No. 702, Aug. 1982.

Magnus, R.; and Yoshihara, H.: Unsteady Transonic Flow Over an Airfoil. AIAA Journal, vol. 13, no. 12, Dec. 1975, pp. 1622-1628.

Pulliam, T. H.: Euler and Thin Layer Navier-Stokes Codes: ARC2D, ARC3D. Notes for Computational Fluid Dynamics User's Workshop, The University of Tennessee Space Institute, Tullahoma, TN, March 1984.

Sorensen, R. L.: A Computer Program to Generate Two-Dimensional Grids About Airfoils and Other Shapes by the Use of Poisson's Equation. NASA TM-81198, May 1980.

Steger, J. L.: Implicit Finite Difference Simulation of Flow About Arbitrary Geometries with Application to Airfoils. AIAA Journal, vol. 16, no. 9, July 1978, pp. 687-692.

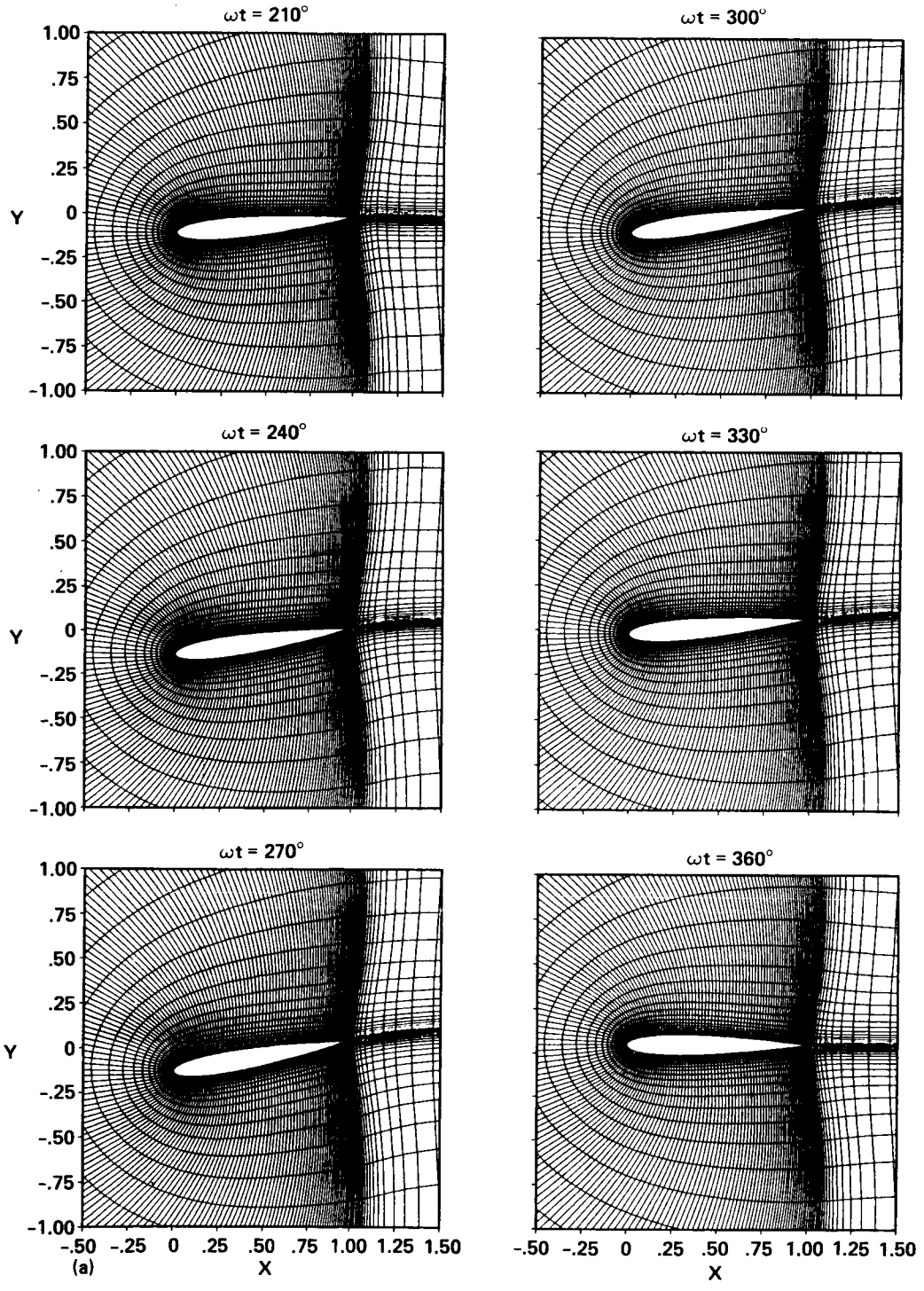

Figure 1.- Demonstration of the moving grid (229 × 48): NACA 0012 heaving-pitching coupled motion.

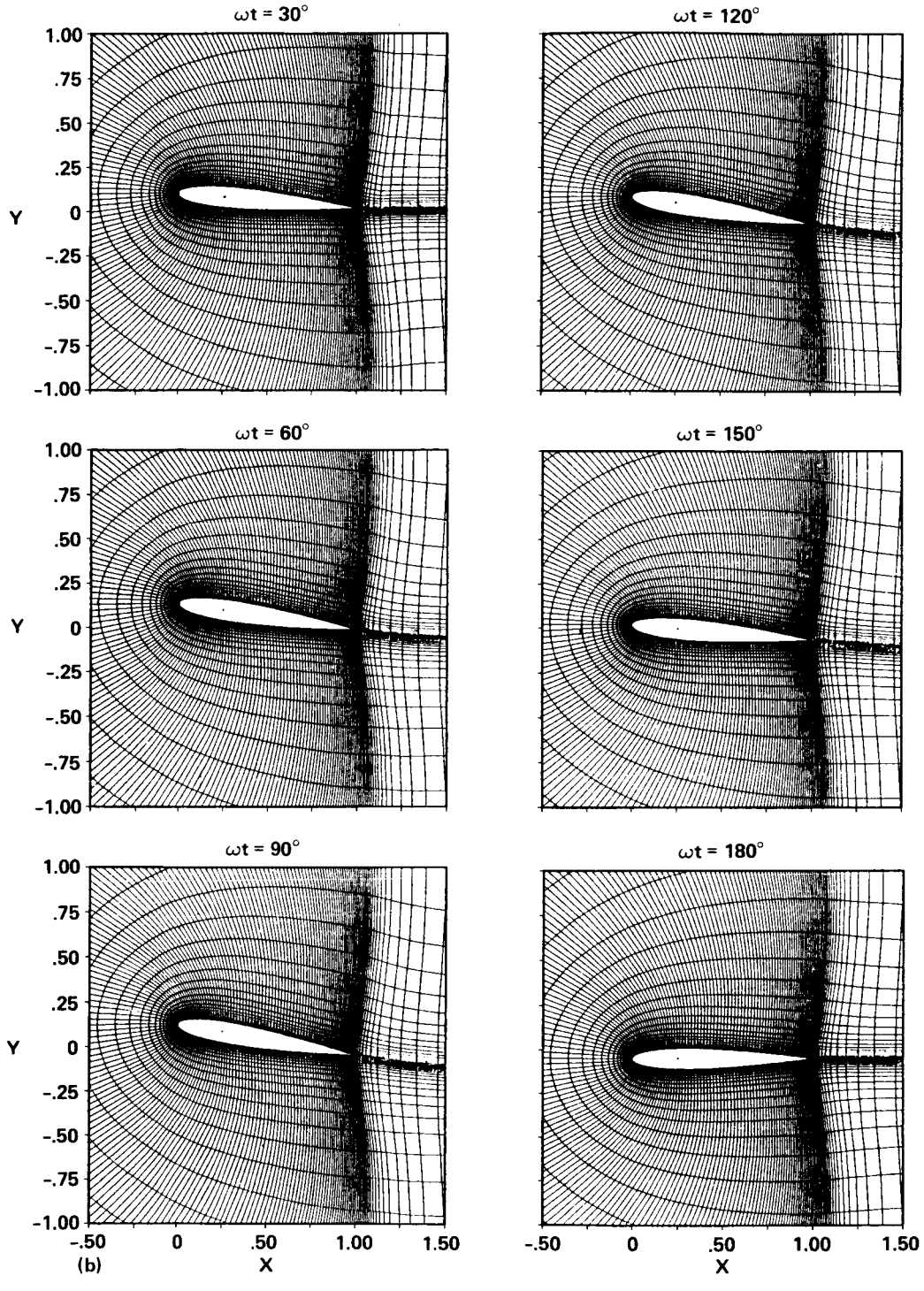

Figure 1.- Concluded.

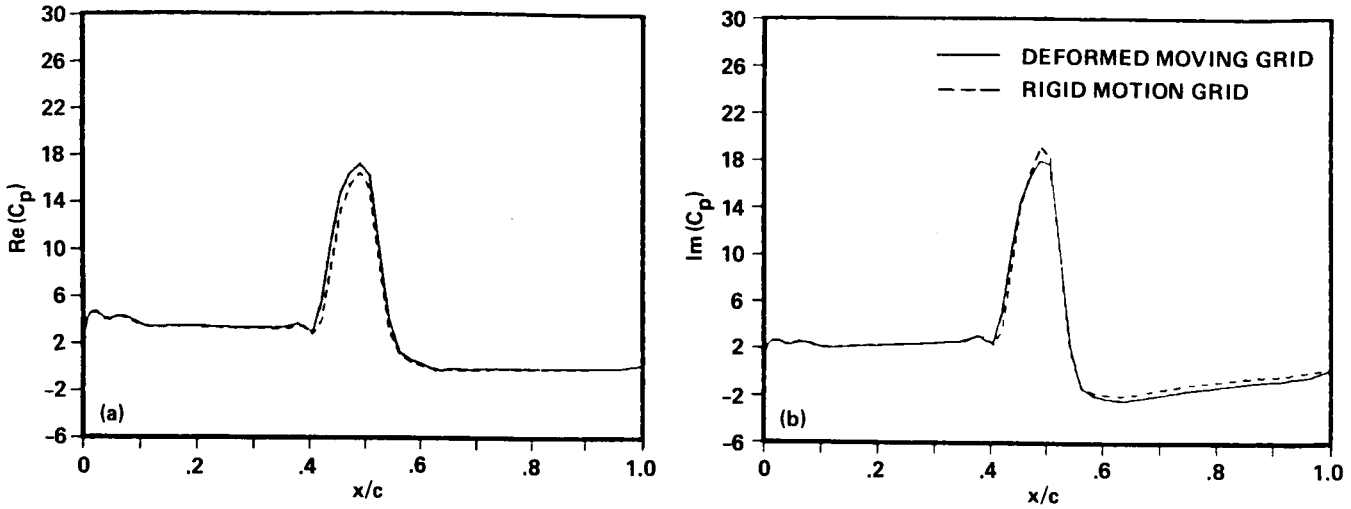

Figure 2.- Comparisons between present grid and rigid motion grid. (a) In-phase (NACA 0012, $M_\infty = 0.8$, $\delta\alpha = 1.0°$, $k = 0.2$). (b) Out-of-phase (NACA 0012, $M_\infty = 0.8$, $\delta\alpha = 1.0°$, $k = 0.2$).

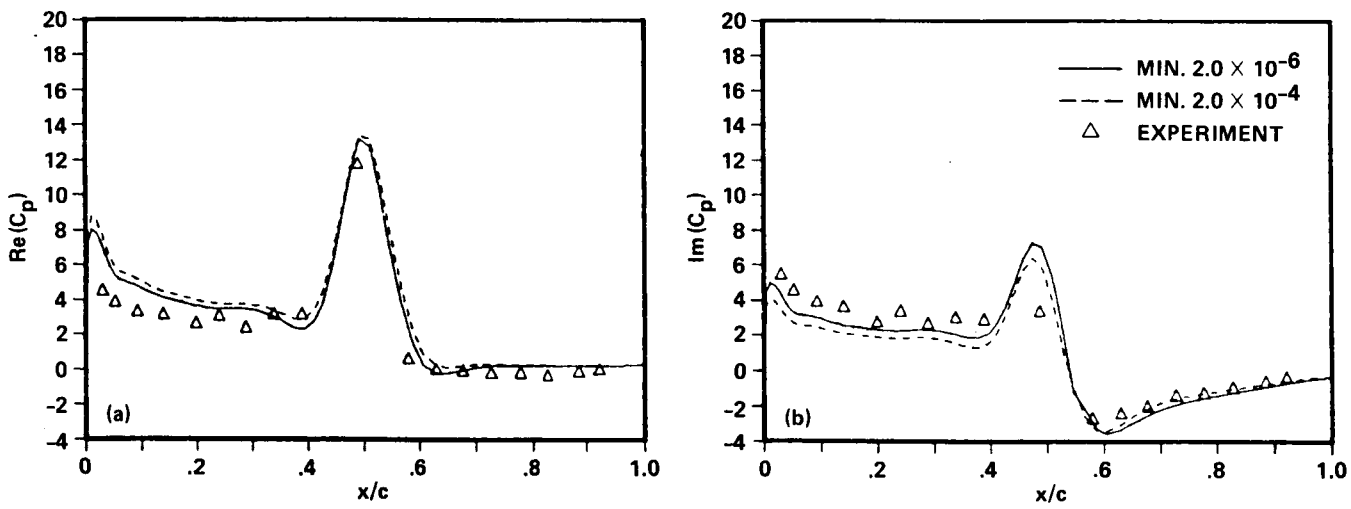

Figure 3.- Effects of minimum grid size on solutions. (a) In-phase (NACA 64A010, $M_\infty = 0.8$, $\delta\alpha = 1.0°$, $k = 0.4$). (b) Out-of-phase (NACA 64A010, $M_\infty = 0.8$, $\delta\alpha = 1.0°$, $k = 0.4$).

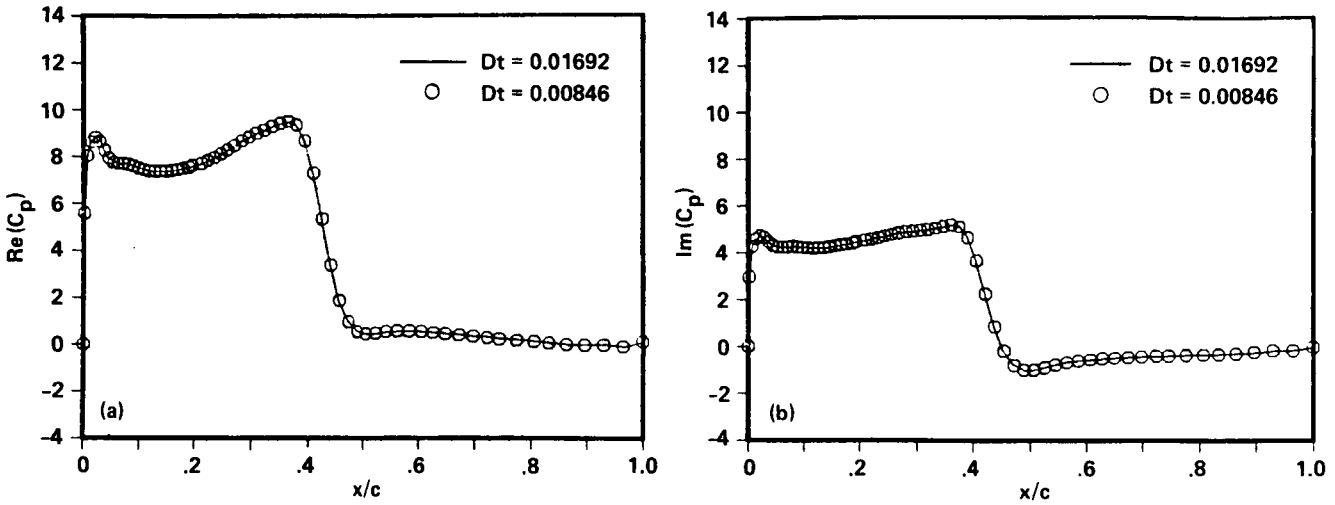

Figure 4.- Effects of time integrating step size on solutions. (a) In-phase (NACA 0012, M_∞ = 0.755, $\delta\alpha$ = 2.51°, k = 0.1628). (b) Out-of-phase (NACA 0012, M_∞ = 0.755, $\delta\alpha$ = 2.51°, k = 0.1628).

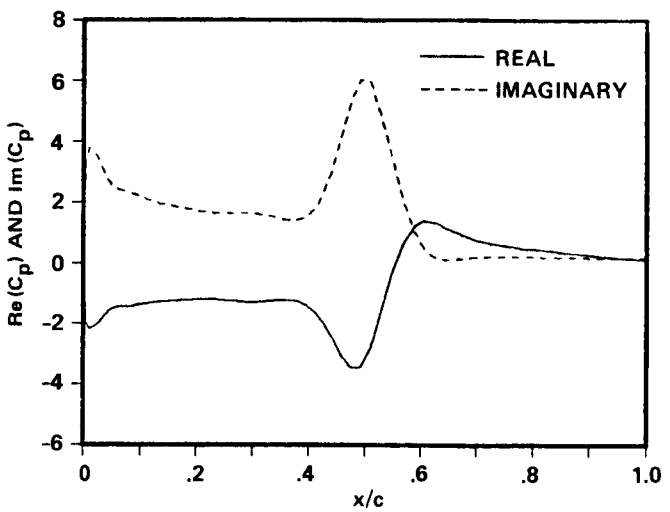

Figure 5.- Unsteady aerodynamics: NACA 64A010 in heaving (M_∞ = 0.8, δh = 0.0436, k = 0.4).

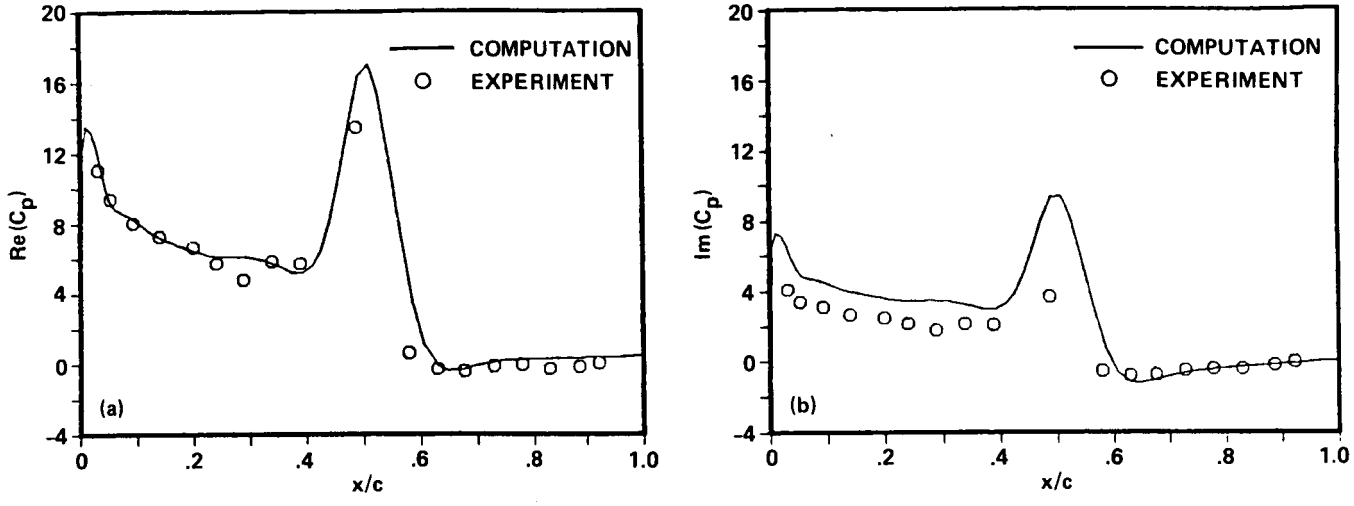

Figure 6.- Unsteady aerodynamics: NACA 64A010 in pitching. (a) In-phase (M_∞ = 0.8, X_a = 0.25, $\delta\alpha$ = 1.0°, k = 0.4). (b) Out-of-phase (M_∞ = 0.8, X_a = 0.25, $\delta\alpha$ = 1.0°, k = 0.4).

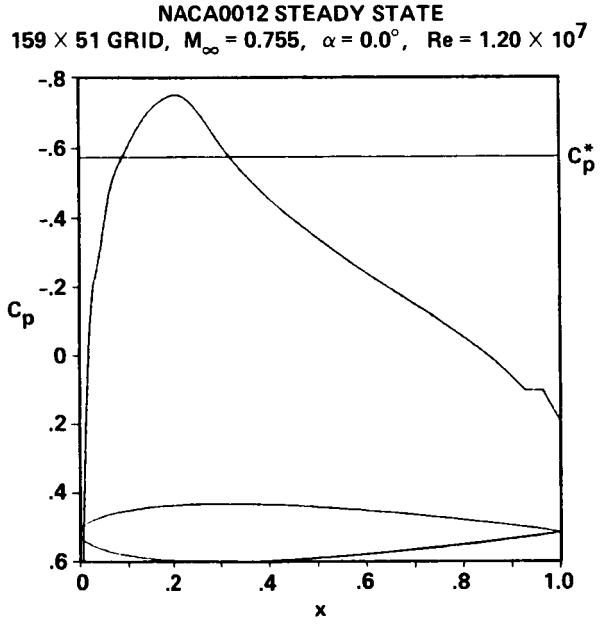

Figure 7.- Steady state solution: NACA 0012 (M_∞ = 0.755, α_m = 0.0°).

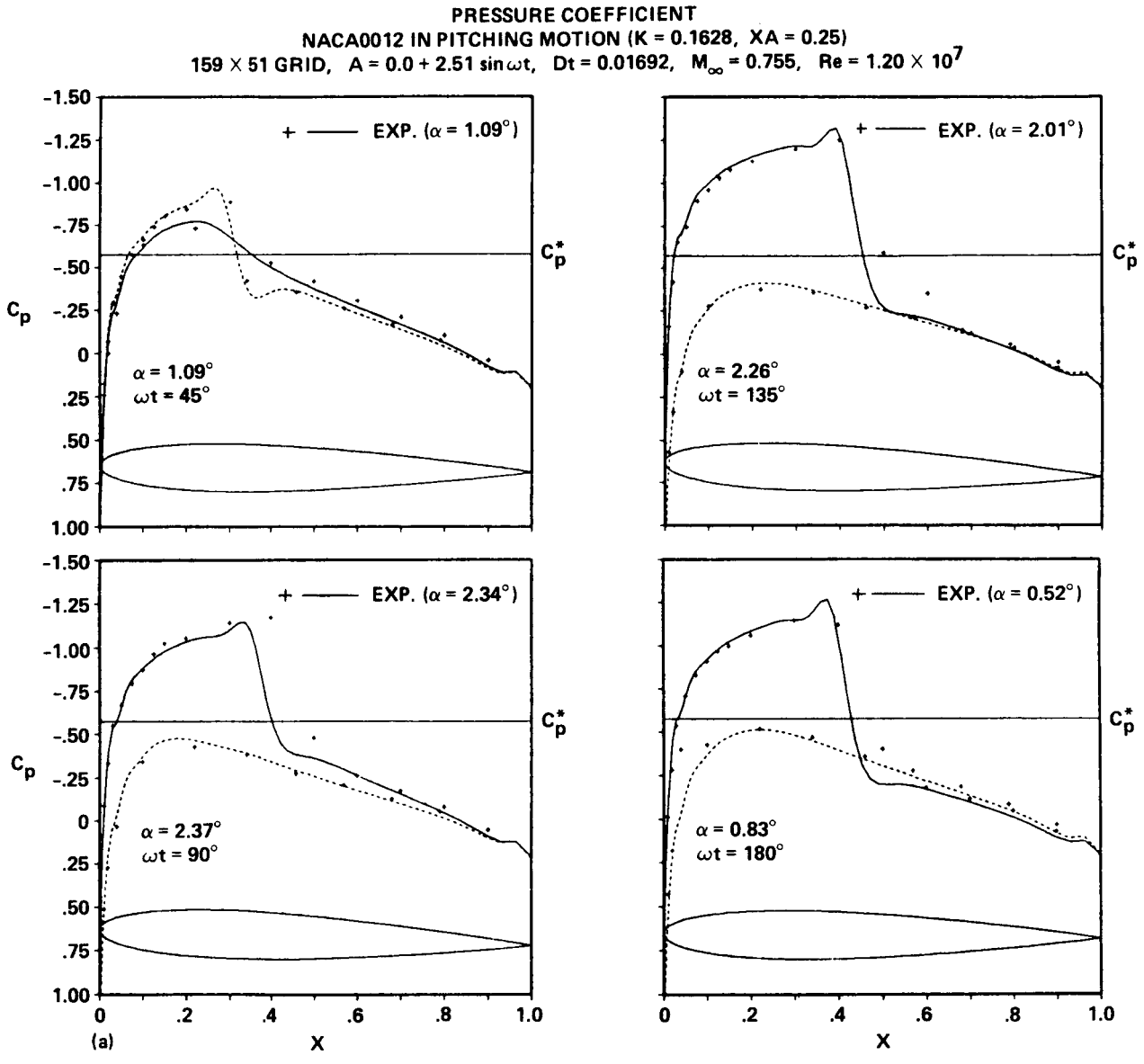

Figure 8.- Time history of C_p distributions: NACA 0012 (M_∞ = 0.755, X_a = 0.5, $\delta\alpha$ = 2.51°, k = 0.1628).

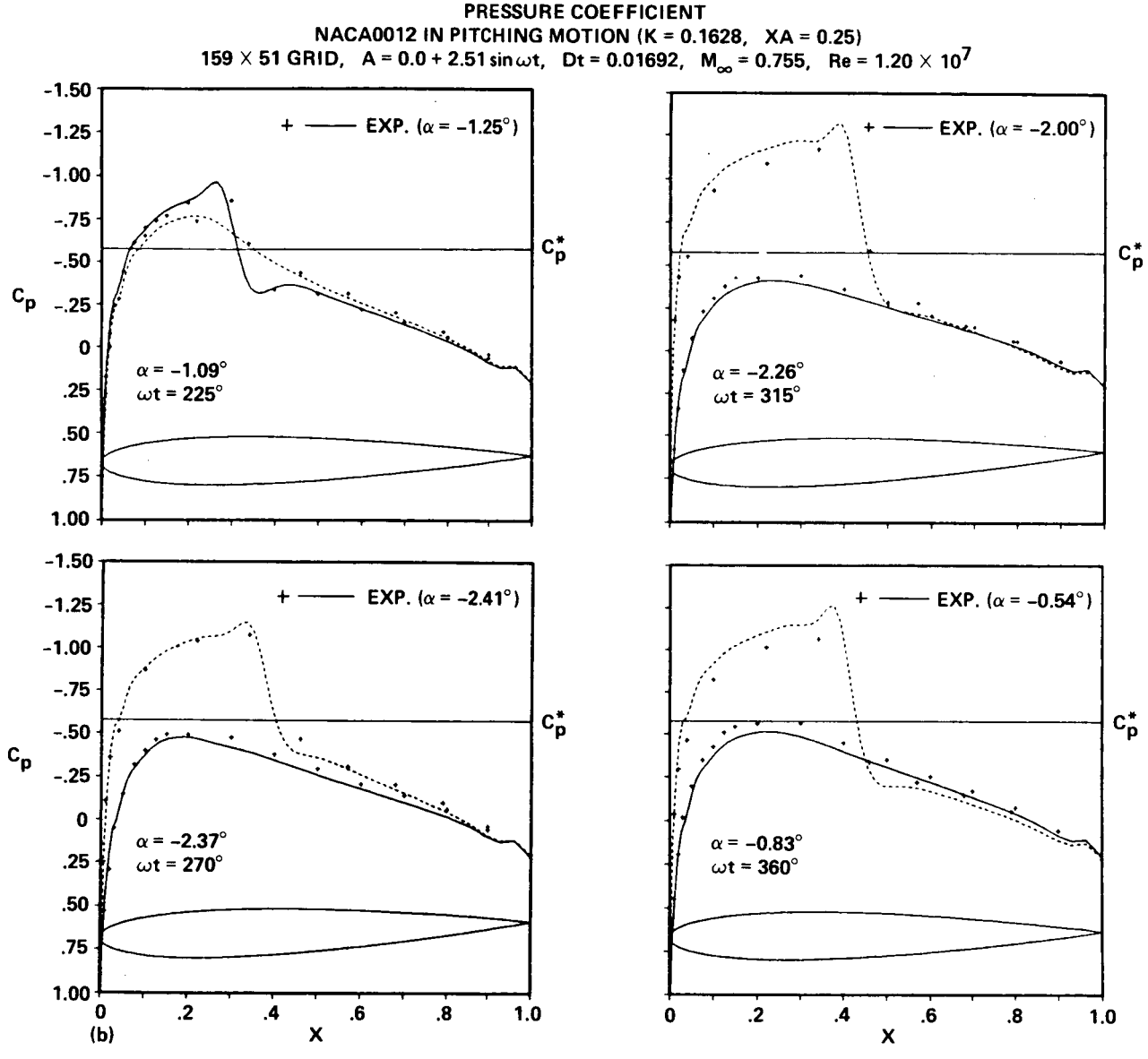

Figure 8.- Concluded.

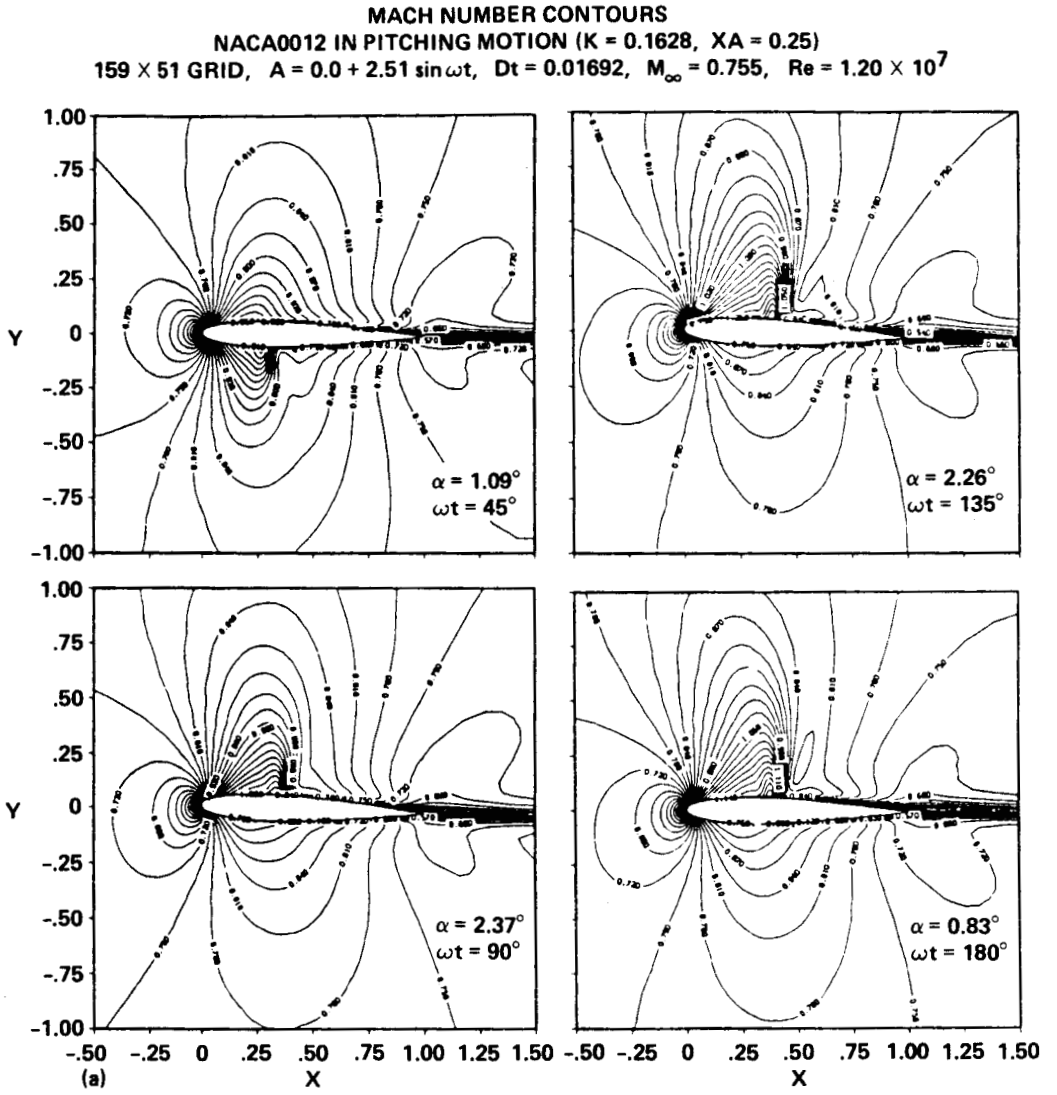

Figure 9.- Time history of Mach contour: NACA 0012 (M_∞ = 0.755, X_a = 0.5, $\delta\alpha$ = 2.51°, k = 0.1628).

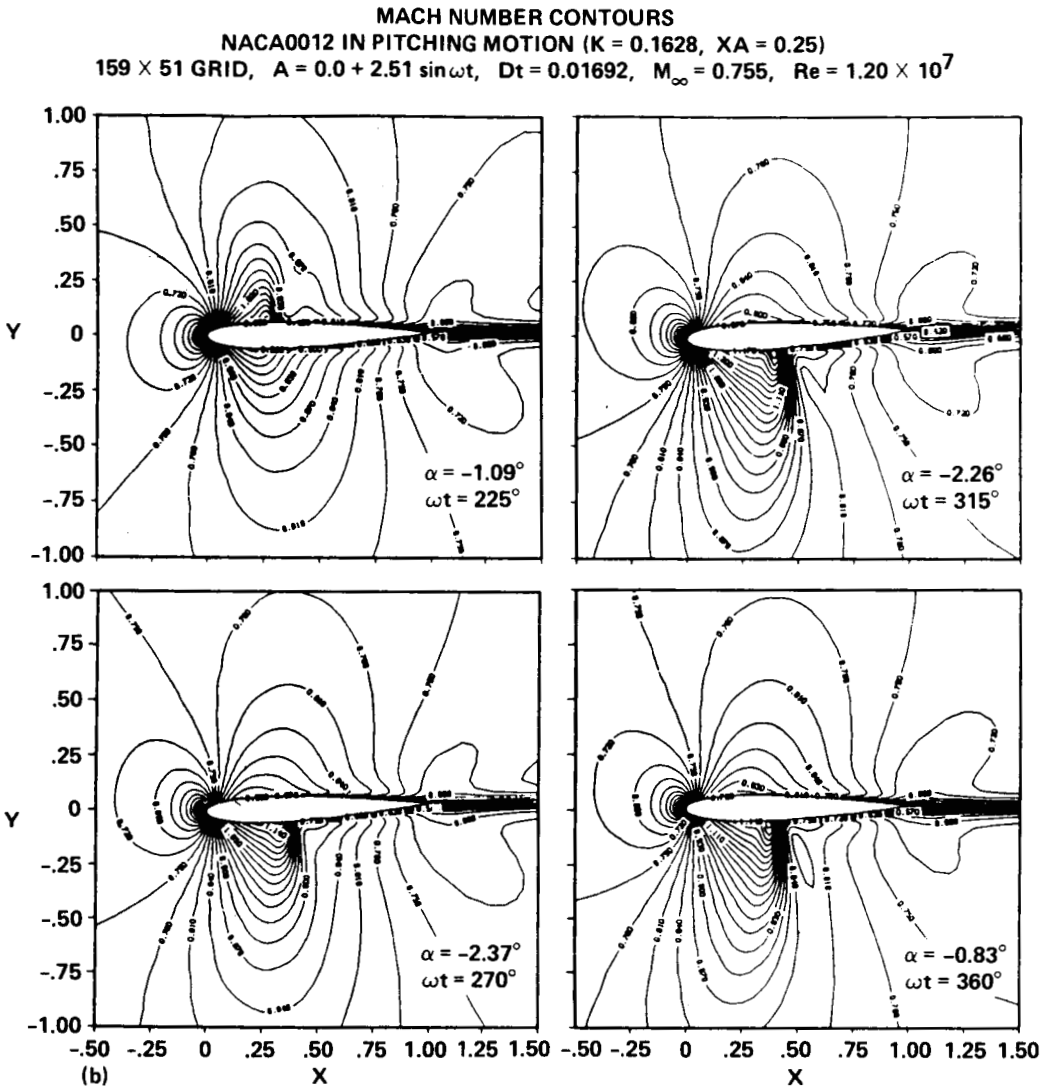

Figure 9.- Concluded.

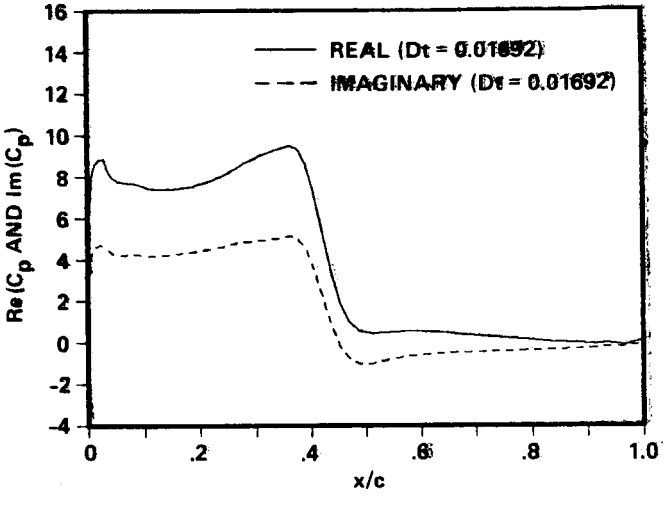

Figure 10.- Unsteady aerodynamics: NACA 0012 in pitching (M_∞ = 0.755, X_a = 0.5, $\delta\alpha$ = 2.51°, k = 0.1628).

1. Report No.	2. Government Accession No.	3. Recipient's Catalog No.
NASA TM-88341		

4. Title and Subtitle	5. Report Date
A VERIFICATION OF UNSTEADY NAVIER-STOKES SOLUTIONS AROUND OSCILLATING AIRFOILS	September 1986
	6. Performing Organization Code: ATP
7. Author(s): Jiro Nakamichi	8. Performing Organization Report No.: A-86337
	10. Work Unit No.
9. Performing Organization Name and Address: Ames Research Center, Moffett Field, CA 94035	11. Contract or Grant No.
	13. Type of Report and Period Covered: Technical Memorandum
12. Sponsoring Agency Name and Address: National Aeronautics and Space Administration, Washington, DC 20546	14. Sponsoring Agency Code: 505-60

15. Supplementary Notes

Point of contact: Mamoru Inouye, Ames Research Center, MS 202A-1, Moffett Field, CA 94035 (415) 694-5126 or FTS 464-5126

16. Abstract

A finite-difference solution code for the two-dimensional Navier-Stokes equations has been combined with a moving-grid system. The thin layer Navier-Stokes equations with a turbulence model are solved in a time-accurate manner in order to study the unsteady aerodynamics around airfoils undergoing small amplitude pitching or heaving motions in the transonic regime. The accuracy of the solutions obtained by the use of the present moving-grid technique is investigated. The effects of the minimum grid size and the integrating time-step size on the solutions are also checked. Some of the solutions obtained by the present method are compared with experimental results.

It is demonstrated that the unsteady aerodynamics around oscillating airfoils can be predicted fairly well by the present code for cases in which the dynamic angle of attack or displacement is small.

17. Key Words (Suggested by Author(s))	18. Distribution Statement
Oscillating airfoils Thin layer Navier-Stokes solutions Moving-grid technique	Unlimited Subject category - 02

19. Security Classif. (of this report)	20. Security Classif. (of this page)	21. No. of Pages	22. Price*
Unclassified	Unclassified	30	A02

*For sale by the National Technical Information Service, Springfield, Virginia 22161